

picture of the field configuration over a much shorter time period (~1 hour).

19. From the measured positions in Fig. 2, a density-distance scale that does not differ significantly from that used earlier (7) can be derived; an approximate  $r^{-2}$  falloff ( $r$  is heliocentric distance) is indicated. These results reinforce the interpretation that the ra-

diation observed by Ulysses occurs at the harmonic of the plasma frequency.

20. J. L. Phillips *et al.*, *Science* **268**, 1030 (1995).  
21. We thank R. F. Benson for many useful suggestions for improving the manuscript.

4 August 1995; accepted 14 September 1995

## Role of Yeast Insulin-Degrading Enzyme Homologs in Propheromone Processing and Bud Site Selection

Neil Adames, Kelly Blundell, Matthew N. Ashby, Charles Boone\*

The *Saccharomyces cerevisiae* *AXL1* gene product Axl1p shares homology with the insulin-degrading enzyme family of endoproteases. Yeast *axl1* mutants showed a defect in **a**-factor pheromone secretion, and a probable site of processing by Axl1p was identified within the **a**-factor precursor. In addition, Axl1p appears to function as a morphogenetic determinant for axial bud site selection. Amino acid substitutions within the presumptive active site of Axl1p caused defects in propheromone processing but failed to perturb bud site selection. Thus, Axl1p has been shown to participate in the dual regulation of distinct signaling pathways, and a member of the insulinase family has been implicated in propeptide processing.

Peptide hormones secreted by higher eukaryotes are synthesized as larger precursors and released in mature form by the action of specific processing proteases (1). Analogous proteolytic maturation occurs for *Saccharomyces cerevisiae* pheromones involved in the mating response of haploid **a** and  $\alpha$  cells (2). The pheromone produced by **a** cells, **a**-factor, is one of a growing number of secreted proteins, such as interleukin-1 $\alpha$  (IL-1 $\alpha$ ), IL-1 $\beta$ , and some fibroblast growth factors (such as FGF-1 and FGF-2) (3), that are processed from precursors before export through a nonclassical secretory pathway. The proteolytic maturation of progenitor **a**-factor (pro-**a**-factor) is not well understood and provides an opportunity to identify novel eukaryotic processing enzymes. Here we present genetic evidence implicating yeast homologs of human insulin-degrading enzyme (hIDE), encoded by *AXL1* and *STE23*, in the specific processing of pro-**a**-factor.

Pro-**a**-factor is encoded by two genes, *MFA1* and *MFA2*, with products that are 36 and 38 amino acids in length, respectively (4, 5). These precursors contain a single copy of the mature **a**-factor peptide, with an NH<sub>2</sub>-terminal extension and a COOH-terminal CAAX consensus sequence (C is cysteine, A is usually aliphatic, and X can be various amino acids). The cysteine residue of

CAAX proteins is isoprenylated within the cytoplasm; such lipid-modified proteins become localized in the membrane, then undergo endoproteolysis of the three terminal AAX residues and methylesterification of the free carboxylate group on the prenylated cysteine (6). The genes encoding most of the enzymes responsible for these modifications have been characterized (7, 8), and mutations in these genes abolish **a**-factor secretion, leading to an **a**-specific mating defect (7, 8). After COOH-terminal processing, the **a**-factor precursor undergoes two sequential NH<sub>2</sub>-terminal endoproteolytic events (8, 9). The final NH<sub>2</sub>-terminal cleavage generates mature **a**-factor, a 12-amino acid lipopeptide (10, 11). Ultimately, the *STE6* product, an adenosine triphosphate-hydrolyzing transport protein related to the mammalian multidrug resistance protein (Mdr1), mediates **a**-factor transport across the cell surface (12).

To identify genes required for pro-**a**-factor maturation, we mutagenized **a** cells and screened for strains that showed a reduced mating efficiency as well as a defect in secreted **a**-factor activity (13). A mutant allele, designated *ste22-1*, identified a novel gene required for normal amounts of secreted **a**-factor activity (Fig. 1A). In crosses to a wild-type  $\alpha$  strain, we found that the sterility cosegregated with this reduced pheromone production and that  $\alpha$  *ste22-1* cells mated with normal efficiency (Fig. 1A). A similar but more severe **a**-specific phenotype was associated with a strain from which the **a**-factor structural genes *MFA1* and *MFA2* were deleted (Fig. 1A). Thus,

*ste22-1* mutants exhibited an **a**-specific mating defect that appeared to be caused by reduced secretion of active pheromone.

We cloned *STE22* by complementation of the mating defect of *ste22-1* cells, using a yeast genomic library. Four plasmids, with overlapping genomic inserts, that complemented both the sterility and the reduced **a**-factor production were isolated. Subcloning and sequence analysis revealed that *STE22* was identical to *AXL1* (14). Thus, *AXL1* rescued the mating defect of *ste22-1* cells (Fig. 1B). The *AXL1* product is required for generation of the axial budding pattern displayed by haploid cells (14) and shares sequence similarity with members of a family of endoproteases whose archetypes are hIDE and *Escherichia coli* protease III (15)—metalloproteases with a preference for small peptide substrates (16, 17). In vivo, hIDE is implicated in the degradation of intracellular insulin, whereas the physiological substrate of protease III remains unknown (16, 17). Another member of the hIDE family, rat *N*-arginine dibasic convertase (NRDC), is proposed to function as a prohormone processing enzyme (18). A highly conserved domain is present in hIDE-like sequences that is likely to be important both for proteolysis and for metal binding (Fig. 2A) (17).

An *axl1::URA3* disruption was constructed (Fig. 2B) and introduced into a diploid strain that was heterozygous for *ste22-1*. Sporulation and tetrad analysis revealed that *axl1::URA3* was tightly linked to *ste22-1* (19). Moreover, the *axl1::URA3* phenotype was comparable to that of *ste22-1* (Fig. 1A). These data confirmed that *ste22-1* was a mutant allele of *AXL1*. Mutations in *AXL1* cause haploid cells to bud with a bipolar pattern that is normally displayed by diploid cells (14). Because the genetic background of the strain we used for the mutant isolation is defective for bud site selection (20), we constructed an *axl1* disruption in a haploid strain normal for axial budding, EG123. This *axl1::URA3* mutant showed both a bipolar budding pattern and a mating defect associated with reduced **a**-factor secretion (19).

Because insulinase homologs can function as specific endoproteases (18), Axl1p may act as a propheromone processing enzyme. We tested an *axl1* mutant for defects in COOH-terminal CAAX-proteolysis and found it to be unaffected (21). To address the possibility that Axl1p is involved in NH<sub>2</sub>-terminal processing, **a**-factor proteins were labeled with [<sup>35</sup>S]cysteine in a pulse-chase protocol, then immunoprecipitated from both intracellular and extracellular fractions and subjected to polyacrylamide gel electrophoresis (PAGE). Three different intracellular **a**-factor peptides were observed in cells containing a functional

N. Adames, K. Blundell, C. Boone, Institute of Molecular Biology and Biochemistry, Simon Fraser University, Burnaby, British Columbia, V5A 1S6, Canada.  
M. N. Ashby, Department of Molecular and Cell Biology, University of California, Berkeley, CA 94720, USA.

\*To whom correspondence should be addressed.

*AXL1* gene (Fig. 2C). The largest form, designated P1, has been assigned to a propheromone molecule with a completely modified COOH-terminus, yet retains an unprocessed NH<sub>2</sub>-terminal extension (Fig. 2D) (8, 9). The P2 propheromone is derived from P1 through proteolytic cleavage

within the NH<sub>2</sub>-terminal domain of the precursor (8, 9). The species designated M corresponds to mature **a**-factor, which results from a second cleavage event within the NH<sub>2</sub>-terminal region of P2 (8, 9). Only the mature pheromone is efficiently exported across the plasma membrane and recov-

ered from the extracellular fraction (8, 9). In *axl1::URA3* cells, the P1 propheromone was processed to the P2 form at a normal rate, but the P2 intermediate was processed inefficiently and remained relatively stable for the duration of the chase period (Fig. 2C). Consequently, *axl1::URA3* mutants produced small amounts of exported pheromone (Fig. 2C). Thus, the sterility of *axl1* cells largely resulted from a defect in P2 propheromone processing and reduced secretion of mature **a**-factor.

Although propheromone processing was greatly impaired, *axl1* mutants were able to secrete residual levels of bioactive **a**-factor (Fig. 1), which implied that *S. cerevisiae* contains a functional homolog of Ax11p. The chromosome XII sequencing project has identified a sequence, L8084.12 (22), which we call *STE23*, encoding a new member of the insulin-degrading enzyme family (Fig. 2A). To assess the function of *STE23*, we created a *ste23Δ::URA3* deletion mutation (23). When introduced into strains with a wild-type *AXL1* gene, the *ste23Δ::URA3* mutation failed to perturb mating efficiency or secreted **a**-factor activity (Fig. 1C). In contrast, experiments with the *axl1::URA3 ste23Δ::URA3* double mutant clearly showed that *ste23Δ::URA3* accentuated both the mating and secreted-pheromone defects of *axl1::URA3* cells (Fig. 1C). Pulse-chase studies indicated that the **a**-factor precursor was processed normally in *ste23Δ::URA3* cells; however, as observed for *axl1::URA3* cells, the *axl1::URA3 ste23Δ::URA3* double mutant accumulated the P2 propheromone intracellularly (19). Thus, our findings are consistent with the possibility that Ste23p is responsible for the residual propheromone processing displayed by *axl1* mutants. We also examined the effect of *ste23Δ::URA3* on bud site selection by means of a microcolony assay and calcofluor staining of bud scars (24). EG123 *ste23Δ::URA3* cells bud with an axial pattern, and the *axl1::URA3 ste23Δ::URA3* double mutant generates the bipolar pattern also observed for *axl1::URA3* cells (19). Therefore, Ste23p does not appear to participate in bud site selection.

Both hIDE and protease III contain a sequence motif with two invariant histidine residues and a glutamate, HXXEH (17). Substitutions for either of the histidine residues cause a loss of proteolytic activity as well as a defect in metal binding (17). The glutamate residue is also important for proteolysis, and by analogy with the function ascribed to a similar motif found in thermolysin, the carboxylate side chain of the glutamate is expected to participate in catalysis (25). By site-specific mutagenesis, we generated three variants of the HXXEH sequence found within Ax11p (Fig. 2A) that correspond to substitutions of the first histidine (*axl1-H68A*), and the glutamate residue (*axl1-*

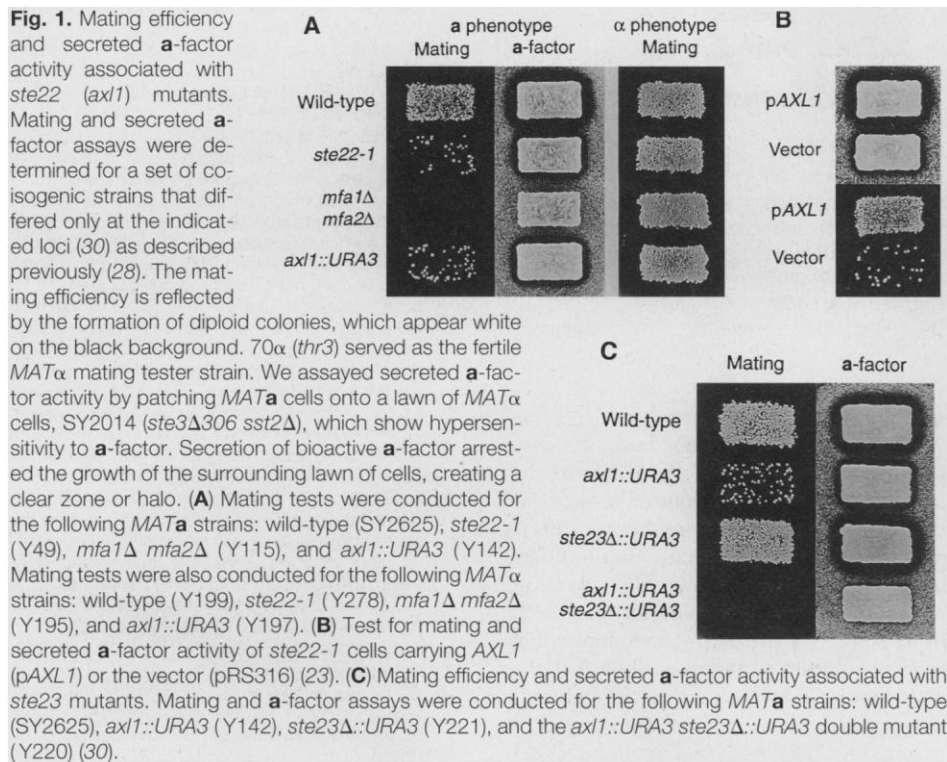


**Fig. 1.** Mating efficiency and secreted **a**-factor activity associated with *ste22* (*axl1*) mutants. Mating and secreted **a**-factor assays were determined for a set of coisogenic strains that differed only at the indicated loci (30) as described previously (28). The mating efficiency is reflected by the formation of diploid colonies, which appear white on the black background. 70 $\alpha$  (*thr3*) served as the fertile MAT $\alpha$  mating tester strain. We assayed secreted **a**-factor activity by patching MAT $\alpha$  cells onto a lawn of MAT $\alpha$  cells, SY2014 (*ste3Δ306 sst2Δ*), which show hypersensitivity to **a**-factor. Secretion of bioactive **a**-factor arrested the growth of the surrounding lawn of cells, creating a clear zone or halo. (A) Mating tests were conducted for the following MAT $\alpha$  strains: wild-type (SY2625), *ste22-1* (Y49), *mfa1Δ mfa2Δ* (Y115), and *axl1::URA3* (Y142). Mating tests were also conducted for the following MAT $\alpha$  strains: wild-type (Y199), *ste22-1* (Y278), *mfa1Δ mfa2Δ* (Y195), and *axl1::URA3* (Y197). (B) Test for mating and secreted **a**-factor activity of *ste22-1* cells carrying *AXL1* (*pAXL1*) or the vector (*pRS316*) (23). (C) Mating efficiency and secreted **a**-factor activity associated with *ste23* mutants. Mating and **a**-factor assays were conducted for the following MAT $\alpha$  strains: wild-type (SY2625), *axl1::URA3* (Y142), *ste23Δ::URA3* (Y221), and the *axl1::URA3 ste23Δ::URA3* double mutant (Y220) (30).

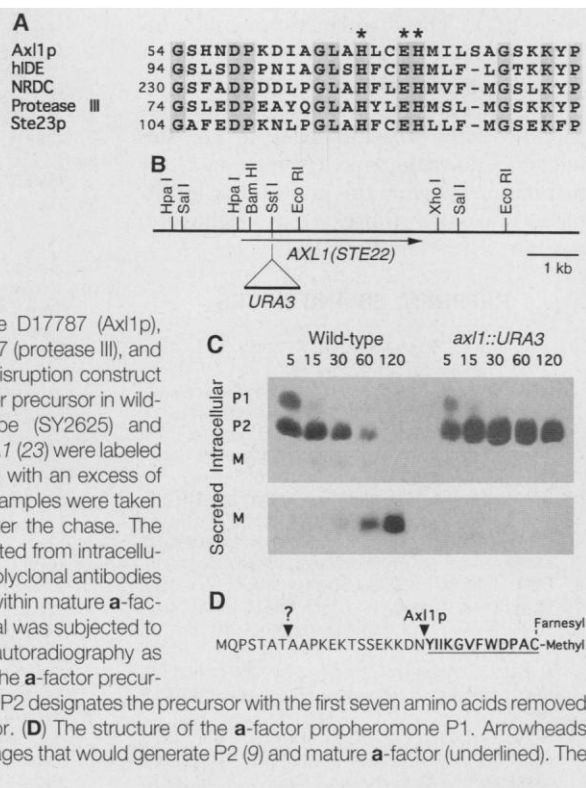
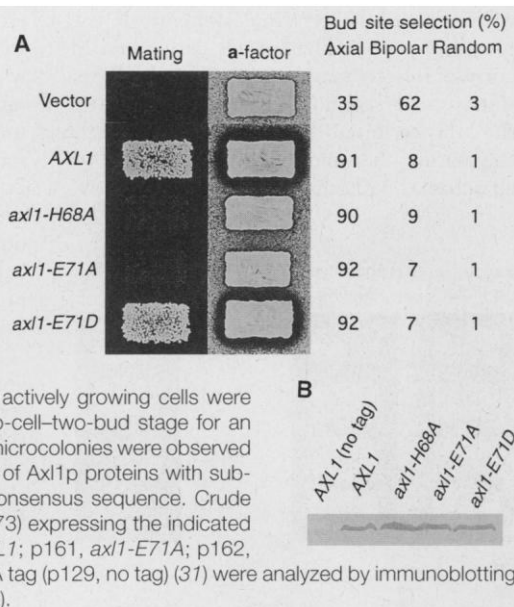


**Fig. 3. (A)** Mating efficiency, secreted  $\alpha$ -factor activity, and bud site selection were determined for  $axl1\Delta::LEU2\ ste23\Delta::LEU2$  double mutant cells carrying substitutions that alter the proposed active site of Axl1p. Cells were transformed with HA epitope-tagged versions of *AXL1*,  $axl1$ -H68A,  $axl1$ -E71A, and  $axl1$ -E71D (p151, p162, p161, and p163, respectively), or with the vector (YEp352) (31). Mating and secreted pheromone assays (28) were conducted with Y231 transformants, and bud site selection assays (24) were conducted with Y272 transformants (30). Before these assays, the cells were grown on selective medium to maintain plasmids. For bud site selection, actively growing cells were spread on agar slabs, and scored at the two-cell-two-bud stage for an axial, bipolar, or random pattern. At least 600 microcolonies were observed for each transformant. **(B)** Steady-state levels of Axl1p proteins with substitutions in the metalloprotease active site consensus sequence. Crude extracts prepared from  $axl1\Delta::LEU2$  cells (Y173) expressing the indicated *AXL1* alleles, either with an HA tag (p151, *AXL1*; p161,  $axl1$ -E71A; p162,  $axl1$ -H68A; p163,  $axl1$ -E71D) or without an HA tag (p129, no tag) (31) were analyzed by immunoblotting with 12CA5 antibodies (Boehringer Mannheim).



*E71A* and  $axl1$ -E71D). Both the  $axl1$ -H68A and  $axl1$ -E71A alleles failed to restore pheromone production and mating to an  $axl1\ ste23$  double mutant, whereas the more conservative substitution associated with  $axl1$ -E71D complemented these mutant phenotypes (Fig. 3A). The loss of function associated with  $axl1$ -H68A and  $axl1$ -E71A was not due to reduced product expression or stability, because epitope-tagged versions of the altered proteins were detected at steady-state levels that were identical to that of the wild-type protein (Fig. 3B). It is likely that Axl1p functions as a metalloprotease involved in propheromone processing with the participation of His<sup>68</sup> and Glu<sup>71</sup> in a thermolysin-like mode of proteolysis.

On the basis of the homology shared with hIDE, it has been suggested that Axl1p contributes to bud site selection through a proteolytic mechanism (14). As a test of this hypothesis, we examined the budding pattern resulting from expression of  $axl1$  alleles altered in the metalloprotease active site consensus sequence. Although defective for  $\alpha$ -factor secretion and mating, we found that cells expressing  $axl1$ -H68A and  $axl1$ -E71A budded with a normal axial pattern (Fig. 3A). Thus, these mutations genetically separated the pheromone processing and bud site selection functions associated with *AXL1*, which suggests that participation of Axl1p in axial budding does not require proteolysis.

We have demonstrated a processing phenotype for  $axl1$  mutants that is consistent with Axl1p acting as a specific endoprotease involved in pro- $\alpha$ -factor maturation. These results combine with those of Fujita *et al.* (14) to implicate *AXL1* in the dual regulation of intercellular signaling during the yeast mating response and intra-

cellular signaling for axial bud site selection. Our findings imply that the proteolytic activity of Axl1p is required to process a farnesylated and membrane-bound form of pro- $\alpha$ -factor (8) to generate mature pheromone for secretion by Ste6p (26); therefore, we suggest that Axl1p may localize to the inner surface of the plasma membrane. Surface localization would also allow Axl1p to contribute to bud site selection through interaction with the products of other genes required for axial budding, including Bud3p and Bud4p, or components of the Rsr1p (Bud1p) Ras-like guanosine triphosphatase cycle (27). These interactions could involve proteolysis, but our results suggest that Axl1p contributes to axial budding through a nonproteolytic mechanism. Regardless of the role for Axl1p in bud site selection, its requirement for pro- $\alpha$ -factor maturation supports the notion that insulinase homologs function as eukaryotic propeptide convertases (18).

## REFERENCES AND NOTES

- D. F. Steiner, S. P. Smeeckens, S. Ohagi, S. J. Chan, *J. Biol. Chem.* **267**, 23435 (1992).
- G. F. Sprague Jr. and J. W. Thorner, in *The Molecular and Cellular Biology of the Yeast Saccharomyces: Gene Expression*, E. W. Jones, J. R. Pringle, J. R. Broach, Eds. (Cold Spring Harbor Laboratory Press, Cold Spring Harbor, NY, 1992), pp. 657-744.
- K. Kuchler and J. Thorner, *Endocrine Rev.* **13**, 499 (1992); I. J. Mason, *Cell* **78**, 547 (1994).
- A. J. Brake, C. Brenner, R. Najarian, P. Laybourn, J. Merryweather, in *Protein Transport and Secretion*, M. J. Gething, Ed. (Cold Spring Harbor Laboratory, Cold Spring Harbor, NY, 1985), pp. 103-108.
- S. Michaelis and I. Herskowitz, *Mol. Cell. Biol.* **8**, 1309 (1988).
- S. Clarke, *Annu. Rev. Biochem.* **61**, 355 (1992); W. R. Schafer and J. Rine, *Annu. Rev. Genet.* **30**, 209 (1992).
- B. He *et al.*, *Proc. Natl. Acad. Sci. U.S.A.* **88**, 11373 (1991); L. E. Goodman *et al.*, *ibid.* **87**, 9665 (1990); M. N. Ashby, D. S. King, J. Rine, *ibid.* **89**, 4613 (1992); R. S. Marr, L. C. Blair, J. Thorner, *J. Biol. Chem.* **265**, 20057 (1990); C. A. Hrycyna and S. Clarke, *Mol. Cell. Biol.* **10**, 5071 (1990); C. A. Hrycyna, S. K. Sapperstein, S. Clarke, S. Michaelis, *EMBO J.* **10**, 1699 (1991); M. N. Ashby, P. R. Errada, V. L. Boyartchuk, J. Rine, *Yeast* **9**, 907 (1993).
- S. Sapperstein, C. Berkower, S. Michaelis, *Mol. Cell. Biol.* **14**, 1438 (1994).
- P. Chen, thesis, Johns Hopkins University School of Medicine, Baltimore, MD (1993).
- R. A. Anderegg, R. Betz, S. A. Carr, J. W. Crabb, W. Duntze, *J. Biol. Chem.* **263**, 18236 (1988); S. Marcus *et al.*, *Mol. Cell. Biol.* **11**, 3603 (1991).
- G. Caldwell *et al.*, *J. Biol. Chem.* **269**, 19817 (1994).
- K. Kuchler, R. E. Sterne, J. Thorner, *EMBO J.* **8**, 3973 (1989); J. P. McGrath and A. Varshavsky, *Nature* **340**, 400 (1989).
- SY2625 (*MATa ura3-1 leu2-3, 112 trp1-1 ade2-1 can1-100 sst1 $\Delta$  mfa2 $\Delta$ ::FUS1-lacZ his3 $\Delta$ ::FUS1-HIS3*) cells were plated onto minimal medium that lacked histidine and contained 0.01 ng of synthetic  $\alpha$ -factor per milliliter (Sigma), then mutagenized to 10% survival by exposure to ultraviolet light and allowed to form colonies. This amount of synthetic  $\alpha$ -factor does not cause G<sub>2</sub> arrest but leads to induced expression of the *FUS1-HIS3* construct, and thereby allows growth of SY2625 on medium lacking histidine. This regime precluded the isolation of mutations that cause reduced signaling of the pheromone response pathway, because such mutations will lead to a slower growth rate on medium lacking histidine. To identify sterile mutants, the mutagenized cells were scored for the ability to mate to 70 $\alpha$  (*thr3*) with the use of a replica-plating procedure (28). Ten mutants that were defective in secreted  $\alpha$ -factor activity (28) were isolated and transformed with plasmids carrying the genes previously known to be involved in pro- $\alpha$ -factor processing. The defects in four mutants were complemented by *STE6*, four were complemented by *RAM1*, and one was complemented by *STE14*.
- A. Fujita *et al.*, *Nature* **372**, 567 (1994).
- J. A. Affolter, V. A. Fried, R. A. Roth, *Science* **242**, 1415 (1988).
- W. C. Duckworth *et al.*, *Biochemistry* **28**, 2471 (1989); L. Ding, A. B. Becker, A. Suzuki, R. A. Roth, *J. Biol. Chem.* **267**, 2414 (1992); A. Anastasi, C. G. Knight, A. J. Barrett, *Biochem. J.* **290**, 601 (1993).
- A. B. Becker and R. A. Roth, *Proc. Natl. Acad. Sci. U.S.A.* **89**, 3835 (1992); *Biochem. J.* **292**, 137 (1993); R. K. Perlman, B. D. Gehm, W. L. Kuo, M. R. Rosner, *J. Biol. Chem.* **268**, 21538 (1993); R. K. Perlman and M. R. Rosner, *ibid.* **269**, 33140 (1994).
- A. Pierotti *et al.*, *Proc. Natl. Acad. Sci. U.S.A.* **91**, 6078 (1994).
- N. Adames, K. Blundell, M. N. Ashby, C. Boone, data not shown.
- F. Cvrckova and K. Nasmyth, *EMBO J.* **12**, 5277 (1993).
- Ras and  $\alpha$ -factor converting enzyme (RACE) assays were done by quantification of the release of the COOH-terminal tritiated tripeptide from the  $\alpha$ -factor-derived peptide KWDPAC(S-trans,trans-farnesyl)[V[4,5-<sup>3</sup>H]IA (29) as described [M. N. Ashby and J. Rine, *Methods Enzymol.* **250**, 235 (1995)]. Protease determinations were made both in 3000g supernatants (S3.0) and 100,000g pellets (P100) in both SY2625 (*AXL1*) and Y49 (*ste22-1*) (30). The *ste22-1* mutation did not substantially affect RACE activity in either cell-free extract. Specific activities were 151 versus 151 pmol/min per milligram for the S3.0 extracts and 250 versus 293 pmol/min per milligram for the P100 extract in SY2625 and Y49, respectively.
- M. Johnston *et al.*, the complete sequence of *Saccharomyces cerevisiae* chromosome XII (in preparation).
- p*AXL1* is a pRS316 plasmid [R. S. Sikorski and P. Hieter, *Genetics* **122**, 19 (1989)] containing an 8.5-kb *AXL1* (*STE22*) genomic fragment, isolated from a yeast genomic library by complementation of the *ste22-1* mating defect [C. Boone, K. L. Clark, G. F. Sprague Jr., *Nucleic Acids Res.* **20**, 4661 (1992)]. Plasmid pSM86 contains *mfa1 $\Delta$ ::LEU2* (5). To create the  $axl1::URA3$  mutation contained on p98, a *URA3* fragment was inserted at the Sst I site, which occurs within a 1-kb Eco RI-Bam HI fragment of *AXL1*, carried on pUC19. The  $axl1::URA3$  mutation alters the

- Axl1p sequence following Ser<sup>206</sup> and occurs within the domain of Axl1p that shows homology with hIDE (14). To delete the complete *STE23* sequence and create the *ste23Δ::URA3* mutation, polymerase chain reaction (PCR) primers (5'-TCGGAAGACCTCAT-TCTTGCTCATT TGGATATGCTC- TGATAGATTG-TACTGAGAGTGCAC-3'; and 5'-GCTACAAACAGC-GTCCGACTTGAATGCCCGCATCTTCGACTGT-GCCGGTATTTACACCGC-3') were used to amplify the *URA3* sequence of pRS316, and the reaction product was transformed into yeast for one-step gene replacement [R. Rothstein, *Methods Enzymol.* **194**, 281 (1991)]. To create the *axl1Δ::LEU2* mutation contained on p114, a 5.0-kb Sal I fragment from pAXL1 was cloned into pUC19, and an internal 4.0-kb Hpa I-Xho I fragment was replaced with a *LEU2* fragment. To construct the *ste23Δ::LEU2* allele (a deletion corresponding to 931 amino acids) carried on p153, a *LEU2* fragment was used to replace the 2.8-kb Pml I-Ecl136 II fragment of *STE23*, which occurs within a 6.2-kb Hind III-Bgl II genomic fragment carried on pSP72 (Promega). To create YEpMFA1, a 1.6-kb Bam HI fragment containing MFA1, from pKK16 [K. Kuchler, R. E. Sterne, J. Thorne, *EMBO J.* **8**, 3973 (1989)], was ligated into the Bam HI site of YEp351 [J. E. Hill, A. M. Myers, T. J. Koerner, A. Tzagoloff, *Yeast* **2**, 163 (1986)].
24. J. Chant and I. Herskowitz, *Cell* **65**, 1203 (1991).
25. B. W. Matthews, *Acc. Chem. Res.* **21**, 333 (1988).
26. K. Kuchler, H. G. Dohlman, J. Thorne, *J. Cell Biol.* **120**, 1203 (1993); R. Kolling and C. P. Hollenberg, *EMBO J.* **13**, 3261 (1994); C. Berkower, D. Loayza, S. Michaelis, *Mol. Biol. Cell* **5**, 1185 (1994).
27. A. Bender and J. R. Pringle, *Proc. Natl. Acad. Sci. U.S.A.* **86**, 9976 (1989); J. Chant, K. Corrado, J. R. Pringle, I. Herskowitz, *Cell* **65**, 1213 (1991); S. Powers, E. Gonzales, T. Christensen, J. Cubert, D. Broek, *ibid.*, p. 1225; H. O. Park, J. Chant, I. Herskowitz, *Nature* **365**, 269 (1993); J. Chant, *Trends Genet.* **10**, 328 (1994); \_\_\_\_\_ and J. R. Pringle, *J. Cell Biol.* **129**, 751 (1995); J. Chant, M. Mischke, E. Mitchell, I. Herskowitz, J. R. Pringle, *ibid.*, p. 767.
28. G. F. Sprague Jr., *Methods. Enzymol.* **194**, 77 (1991).
29. Single-letter abbreviations for the amino acid residues are as follows: A, Ala; C, Cys; D, Asp; E, Glu; F, Phe; G, Gly; H, His; I, Ile; K, Lys; L, Leu; M, Met; N, Asn; P, Pro; Q, Gln; R, Arg; S, Ser; T, Thr; V, Val; W, Trp; and Y, Tyr.
30. A W303 1A derivative, SY2625 (*MATα ura3-1 leu2-3, 112 trp1-1 ade2-1 can1-100 sst1Δ mfa2Δ::FUS1-lacZ his3Δ::FUS1-HIS3*), was the parent strain for the mutant search. SY2625 derivatives for the mating assays, secreted pheromone assays, and the pulse-chase experiments included the following strains: Y49 (*ste22-1*), Y115 (*mfa1Δ::LEU2*), Y142 (*axl1::URA3*), Y173 (*axl1Δ::LEU2*), Y220 (*axl1::URA3 ste23Δ::URA3*), Y221 (*ste23Δ::URA3*), Y231 (*axl1Δ::LEU2 ste23Δ::LEU2*), and Y233 (*ste23Δ::LEU2*). *MATα* derivatives of SY2625 included the following strains: Y199 (SY2625 made *MATα*), Y278 (*ste22-1*), Y195 (*mfa1Δ::LEU2*), Y196 (*axl1Δ::LEU2*), and Y197 (*axl1::URA3*). The EG123 (*MATα leu2 ura3 trp1 can1 his4*) genetic background was used to create a set of strains for analysis of bud site selection. EG123 derivatives included the following strains: Y175 (*axl1Δ::LEU2*), Y223 (*axl1::URA3*), Y234 (*ste23Δ::LEU2*), and Y272 (*axl1Δ::LEU2 ste23Δ::LEU2*). *MATα* derivatives of EG123 included the following strains: Y214 (EG123 made *MATα*) and Y293 (*axl1Δ::LEU2*). All strains were generated by means of standard genetic or molecular methods involving the appropriate constructs (23). In particular, the *axl1 ste23* double mutant strains were created by crossing of the appropriate *MATα ste23* and *MATα axl1* mutants, followed by sporulation of the resultant diploid and isolation of the double mutant from nonparental di-type tetrads. Gene disruptions were confirmed with either PCR or Southern (DNA) analysis.
31. p129 is a YEp352 [J. E. Hill, A. M. Myers, T. J. Koerner, A. Tzagoloff, *Yeast* **2**, 163 (1986)] plasmid containing a 5.5-kb Sal I fragment of pAXL1. p151 was derived from p129 by insertion of a linker at the Bgl II site within *AXL1*, which led to an in-frame insertion of the hemagglutinin (HA) epitope (DQYPYDVPDYA) (29) between amino acids 854 and 855 of the *AXL1* protein. pC225 is a KS+ (Stratagene) plasmid containing a 0.5-kb Bam HI-Sst I fragment from pAXL1. Substitution mutations of the proposed active site of Axl1p were created with the use of pC225 and site-specific mutagenesis involving appropriate synthetic oligonucleotides (*axl1-H68A*, 5'-GTGCTCACAAAGCGCTGCCAAACCGGC-3'; *axl1-E71A*, 5'-AAGAATCATGTGCGCACAAAGGTGCGC-3'; and *axl1-E71D*, 5'-AAGAATCATGTGATCACAAAGGTGCGC-3'). The mutations were confirmed by sequence analysis. After mutagenesis, the 0.4-kb Bam HI-Msc I fragment from the mutagenized pC225 plasmids was transferred into pAXL1 to create a set of pRS316 plasmids carrying different *AXL1* alleles, p124 (*axl1-H68A*), p130 (*axl1-E71A*), and p132 (*axl1-E71D*). Similarly, a set of HA-tagged alleles carried on YEp352 were created after replacement of the p151 Bam HI-Msc I fragment, to generate p161 (*axl1-E71A*), p162 (*axl1-H68A*), and p163 (*axl1-E71D*).
32. We thank J. Becker and S. Michaelis for providing a-factor antibodies; S. Michaelis for discussing unpublished results and helping with the pulse-chase experiments; J. Brown, J. Chant, and S. Sanders for their input concerning bud site selection experiments; M. Raymond, F. Taminoi, and M. Whiteway for plasmids; M. Marra for providing the *STE23* genomic fragment; and H. Bussey, J. Brown, N. Davis, T. Favero, C. de Hoog, and S. Kim for comments on the manuscript. Supported by a grant to C.B. from the Natural Sciences and Engineering Research Council of Canada. Support for M.N.A. was from a California Tobacco-Related Disease Research Program postdoctoral fellowship (4FT-0083).

22 June 1995; accepted 21 August 1995

## Quantitative Monitoring of Gene Expression Patterns with a Complementary DNA Microarray

Mark Schena,\* Dari Shalon,\*† Ronald W. Davis, Patrick O. Brown‡

A high-capacity system was developed to monitor the expression of many genes in parallel. Microarrays prepared by high-speed robotic printing of complementary DNAs on glass were used for quantitative expression measurements of the corresponding genes. Because of the small format and high density of the arrays, hybridization volumes of 2 microliters could be used that enabled detection of rare transcripts in probe mixtures derived from 2 micrograms of total cellular messenger RNA. Differential expression measurements of 45 *Arabidopsis* genes were made by means of simultaneous, two-color fluorescence hybridization.

The temporal, developmental, topographical, histological, and physiological patterns in which a gene is expressed provide clues to its biological role. The large and expanding database of complementary DNA (cDNA) sequences from many organisms (1) presents the opportunity of defining these patterns at the level of the whole genome.

For these studies, we used the small flowering plant *Arabidopsis thaliana* as a model organism. *Arabidopsis* possesses many advantages for gene expression analysis, including the fact that it has the smallest genome of any higher eukaryote examined to date (2). Forty-five cloned *Arabidopsis* cDNAs (Table 1), including 14 complete sequences and 31 expressed sequence tags (ESTs), were used as gene-specific targets. We obtained the ESTs by selecting cDNA clones at random from an *Arabidopsis* cDNA library. Sequence analysis revealed that 28 of the 31 ESTs matched sequences

in the database (Table 1). Three additional cDNAs from other organisms served as controls in the experiments.

The 48 cDNAs, averaging ~1.0 kb, were amplified with the polymerase chain reaction (PCR) and deposited into individual wells of a 96-well microtiter plate. Each sample was duplicated in two adjacent wells to allow the reproducibility of the arraying and hybridization process to be tested. Samples from the microtiter plate were printed onto glass microscope slides in an area measuring 3.5 mm by 5.5 mm with the use of a high-speed arraying machine (3). The arrays were processed by chemical and heat treatment to attach the DNA sequences to the glass surface and denature them (3). Three arrays, printed in a single lot, were used for the experiments here. A single microtiter plate of PCR products provides sufficient material to print at least 500 arrays.

Fluorescent probes were prepared from total *Arabidopsis* mRNA (4) by a single round of reverse transcription (5). The *Arabidopsis* mRNA was supplemented with human acetylcholine receptor (AChR) mRNA at a dilution of 1:10,000 (w/w) before cDNA synthesis, to provide an internal standard for calibration (5). The resulting fluorescently labeled cDNA mixture was hybridized to an array at high stringency (6) and scanned

M. Schena and R. W. Davis, Department of Biochemistry, Beckman Center, Stanford University Medical Center, Stanford, CA 94305, USA.

D. Shalon and P. O. Brown, Department of Biochemistry and Howard Hughes Medical Institute, Beckman Center, Stanford University Medical Center, Stanford, CA 94305, USA.

\*These authors contributed equally to this work.

†Present address: Synteni, Palo Alto, CA 94303, USA.

‡To whom correspondence should be addressed. E-mail: pbrown@cmgm.stanford.edu